Modelling the Potential Impacts of Climate Change on Snowpack in the North Saskatchewan River Watershed, Alberta

Ryan J. MacDonald · James M. Byrne · Sarah Boon · Stefan W. Kienzle

Abstract The North Saskatchewan River basin is a large watershed in central Alberta that provides water for a range of stakeholders, including large municipalities, agricultural operations, power generation, and resource extraction industries. This study assesses potential future changes in snowpack for the North Saskatchewan River watershed in response to a range of GCM-derived climate warming scenarios representing the periods from 2010-2039 (2020s), 2040-2069 (2050s), and 2070-2099 (2080s). The GENESYS (GENerate Earth SYstems Science input) spatial hydrometeorological model is applied to simulate potential changes in the zero degree isotherm, precipitation phase, watershed average maximum spring snow water equivalent (SWE), the dates of maximum and minimum SWE, and snowmelt period for these future climate scenarios. Climate warming is likely to result in an upwards shift in elevation of the zero degree isotherm, with a transition to more precipitation occurring as rain than snow. Although watershed average maximum SWE may not change under future conditions, the timing of spring snowmelt onset is likely to change under the future climate scenarios applied. It is demonstrated that increased air temperatures are expected to result in substantial changes in snowpack processes in the North Saskatchewan River watershed.

Keywords Climate change · Snowpack · Mountain hydrology

1 Introduction

Mountainous regions are the main water source for many of the world's river systems (Beniston et al. 1997). Changes in mountain snowpack have been observed across North America (Cayan et al. 2001; Mote et al. 2005; Stewart 2009), with up to 60 % of climate-related trends over the Western United States from 1950 to 1999 attributed to human-induced climate warming (Barnett et al. 2008). Mountain snow accumulation is expected to decline with continued atmospheric warming (Beniston 2003; Hamlet and Lettenmaier

R. J. MacDonald · J. M. Byrne (✉) · S. Boon · S. W. Kienzle
Department of Geography, University of Lethbridge, 4401 University Drive, Lethbridge, Alberta, Canada
T1K 3M4
e-mail: byrne@uleth.ca

1999; Lapp et al. 2005), reducing snowmelt contributions to streamflow in mountainous regions (Barnett et al. 2005). These changes, compounded by enhanced landscape disturbance due to wildfire and pest outbreaks (Flannigan et al. 2005; Hicke and Jenkins 2008; Littell et al. 2009) would significantly affect water supply from snow dominated regions. This anticipated reduction in available water for both human and ecosystem needs poses a substantial challenge for future water resource management (Harma et al. 2011).

Numerous studies have documented hydrological changes in snow dominated regions, including earlier melt onset (Cayan et al. 2001; Mote et al. 2005; Stewart et al. 2004; Stewart et al. 2005; Stewart 2009; Clow 2010) and decreases in mean annual streamflow (Zhang et al. 2001; Rood et al. 2005; St. Jaques et al. 2010). However, few studies have quantified the potential future impacts of climate change on snowpack for the eastern slopes of the Canadian Rocky Mountains (Cohen 1991; Lapp et al. 2005; Valeo et al. 2007).

Snowpack from watersheds on the eastern slopes of the Canadian Rocky Mountains is an important source of water for the western prairie provinces of Alberta, Saskatchewan and Manitoba (Schindler and Donahue 2006), particularly from the North Saskatchewan watershed. This watershed is subject to the 1969 Master Agreement on Apportionment, which dictates that Alberta must allow 50 % of the annual natural flow to enter the province of Saskatchewan, while maintaining minimum in-stream flow requirements (North Saskatchewan Watershed 2005). In addition to maintaining adequate streamflow for downstream users, reservoir operations on the upper North Saskatchewan are at risk, as the reliability of reservoirs could decrease under future climate change (Minville et al. 2009; Minville et al. 2010). In order to adequately manage this system, it is important to understand how snowpack in the North Saskatchewan headwaters may change in the future.

We quantify potential changes in SWE in the North Saskatchewan River watershed for the 2020s (2010-39), 2050s (2040-69), and 2080s (2070-99) relative to the historical 1961 to 1990 period, by applying a range of future climate scenarios to a high resolution hydrometeorological model. Model outputs are analyzed to define potential changes in the zero degree isotherm and shifts in the proportion of precipitation falling as snow. Potential changes in annual maximum basin SWE (mm) and spatial changes in the timing of maximum and minimum SWE (days) are also quantified for the entire watershed.

2 Study Area

The study area comprises the mountain headwater region of the North Saskatchewan River watershed originating at the Columbia Icefield, as well as the foothills region east of the Rocky Mountains (Fig. 1). This 20,527 km^2 portion of the North Saskatchewan River watershed contributes the majority of streamflow to the North Saskatchewan system, and constitutes the total contributing area for all hydroelectric generation upstream of Edmonton, Alberta.

The study region is characterized by a cool, wet continental climate. At the Bighorn climate station, located in the center of the watershed, normal (1971 to 2000) annual air temperature was 2.7 °C and average annual total precipitation was 493 mm (Environment Canada 2010; Table 1). The watershed is characterized as topographically diverse, with an elevation range from 752 m to 3184 m (Fig. 2). The study region is densely vegetated; with 56 % of the watershed area covered by coniferous, 5 % deciduous, and 2 % mixed forest. The remaining 37 % of the region is crop land, grassland, shrubland and glacier (Circa, 2000). In 2000, 1.5 % of the study region was glaciated and contained an estimated 21 km^3 of active glacial ice (Booth et al. 2010). The geology of the North Saskatchewan River headwaters is comprised primarily of Triassic to Tertiary shale and sandstone (Gadd 1995). A range of land uses are present including forestry, mining,
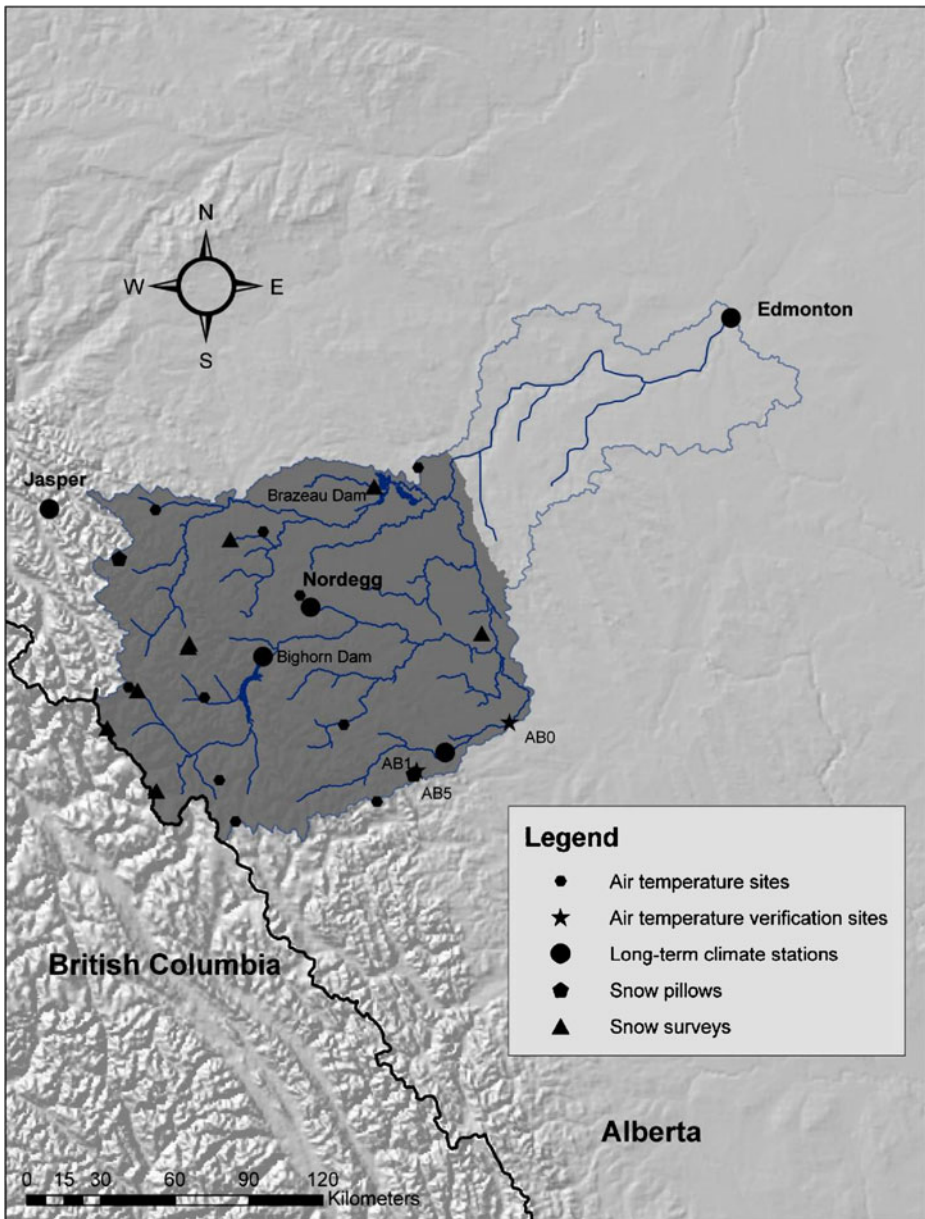
Fig. 1 Upper North Saskatchewan River watershed, Alberta, Canada. Locations of air temperature and snow data sites used in the modelling are identified

petrochemical operations, and hydro electric generation. The hydro electric industry is heavily reliant on streamflow, as the Bighorn and Brazeau Dams on the Bighorn and Brazeau Rivers have the capacity to produce approximately 408, 000 and 397, 000 MWh, respectively, on an annual basis (Transalta 2009). In addition to hydro electric power generation, the North Saskatchewan River provides drinking water for several downstream urban areas, including the Edmonton Metropolitan region with a population of 1.1 million (City of Edmonton 2010).

Table 1 Normal (1971–2000) monthly and annual air temperature (°C) and precipitation (mm) for the Bighorn climate station located in the center of the study area

	Jan	Feb	Mar	Apr	May	Jun	Jul	Aug	Sep	Oct	Nov	Dec	Annual
Air temperature (°C)	−9.1	−6.3	−2.7	2.8	7.5	11.5	14.0	13.3	8.7	3.8	−3.7	−7.3	2.7
Precipitation (mm)	24.1	15.0	19.4	27.1	62.6	76.6	76.9	70.4	53.1	30.0	18.3	19.8	493.0

3 Methods

3.1 Meteorological Data

Three Environment Canada climate stations: Nordegg (1320 meters above sea level (m)), Bighorn Dam (1341 m), and Clearwater (1280 m), provided daily air temperature and precipitation input data to drive the model (Table 2, Fig. 1). A continuous daily air temperature and precipitation time series from 1960 to 2008 was created for each of the three driver stations by infilling data gaps for 25 %, 20 %, and 31 % of the records for the Bighorn, Nordegg and Clearwater climate stations, respectively. This was completed using linear relationships derived between each station and other nearby climate stations.

For model calibration and validation, air temperature data were available at 12 sites which were either fire lookout towers or meteorological stations (Table 2, Fig. 1). These 12 sites ranged in elevation from 1070 to 2316 m, and recorded data for varying time periods between 1976 and 2007 (Alberta Environment 2009; Smith 2009). SWE data from 11 snow survey sites (Table 2, Fig. 1) with at least one measurement per year for the 1978–2008 period were also obtained from Alberta Environment (Alberta Environment 2009). SWE data from three more recently installed snow survey sites were also obtained for the 2002 to 2006 period from the Foothills Orographic Precipitation Experiment (Smith 2009). Daily SWE data (2001 to 2008) from two snow pillows at Limestone Ridge and Southesk (Table 2, Fig. 1) were also obtained from Alberta Environment (Alberta Environment 2009). Both snow pillows are located in clearings within open spruce
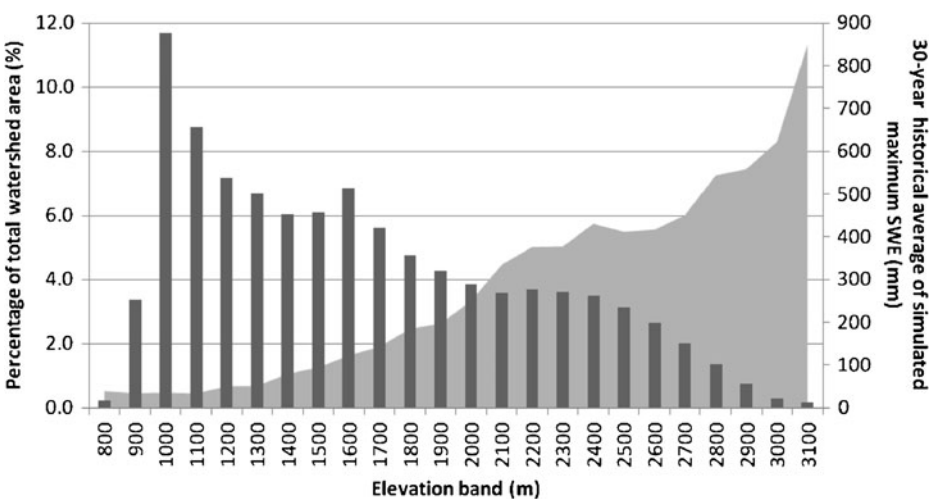
Fig. 2 Percentage of watershed area (bars) and 30-year historical average of simulated maximum SWE (grey area) for all elevation bands

Table 2 Summary of air temperature and SWE data used

Name	Elevation (m)	Observed Time Period	Observed Variable
(AE) Bow Summit	2080	1998–2007	Air temperature
Baldy LO	2083	1960–2007	Air temperature
Cline LO	2050	1975–2007	Air temperature
Grave Flatts LO	2074	1960–2007	Air temperature
Parker Ridge	2023	1978–2007	Air temperature
Ram Falls	1641	1989–2007	Air temperature
Sask River Crossing 2	1392	1976–2007	Air temperature
Scalp Creek	2042	1982–2007	Air temperature
Upper Parker Ridge	2317	1998–2007	Air temperature
Brazeau Reservoir	970	1977–2008	SWE
Brown Creek	1340	1977–2008	SWE
Crimson Lake	970	1973–2007	SWE
Golden Eagle	2090	1985–2008	SWE
Job Creek 1	2100	1985–2008	SWE
Job Creek 2	2005	1993–2008	SWE
Limestone Ridge	1950	1983–2008	SWE
Limestone Snowpillow	1950	2001–2008	SWE
Nigel Creek	1920	1968–2008	SWE
Nordegg	1465	1974–2008	SWE
Southesk	2200	1986–2008	SWE
Southesk Snowpillow	2200	2006–2008	SWE
Watchman Creek	1830	1985–2002	SWE
Caroline (AB0)	1070	2002–2006	SWE/Air temperature
Clearwater RS (AB1)	1280	2002–2006	SWE/Air temperature
Limestone West (AB5)	2120	2002–2006	SWE/Air temperature

forests (J. Pedlar and R. Pickering, Alberta Environment, pers. comm.). Given data gaps in these records, however, only years with complete time series were used to validate modelled SWE (Limestone Ridge: 2001–2007; Southesk: 2007–2008).

3.2 Air Temperature and Precipitation

Monthly maximum and minimum air temperature lapse rates were used to estimate daily air temperature as a function of elevation and month. The initial temperature simulations applied maximum and minimum air temperature lapse rates derived from the Parameter Elevation Regression on Independent Slopes Model (PRISM) 1971 to 2000 monthly normal temperature grids (Daly et al. 2008). Application of these lapse rates resulted in over simulations of both maximum and minimum air temperatures. The derived PRISM lapse rates were then calibrated to measured monthly average maximum and minimum air temperatures by iteratively changing the lapse rate to minimize the difference between observed and simulated monthly air temperature values at eight high elevation fire stations (Fig. 1 and Table 2). The resultant lapse rates for each month are presented in Table 3. These monthly lapse rates were applied to daily temperature values at the driver stations to predict air temperature over the study area based on elevation change from the driver station. Three

Table 3 Monthly calibrated lapse rates for maximum and minimum temperature (°C km^{-1})

	Jan	Feb	Mar	Apr	May	Jun	Jul	Aug	Sep	Oct	Nov	Dec
Tmax	5.9	5.8	5.7	6.4	6.7	7.6	6.6	6.2	6.0	7.5	6.7	6.8
Tmin	0.4	0.3	3.6	4.5	3.7	4.9	4.4	3.3	2.1	2.6	2.3	0.9

Alberta Environment temperature sites (AB 0, AB 1, AB 5) ranging in elevation from 1070 to 2120 m were used to validate the simulated daily air temperature values (Table 1, Fig. 1).

To estimate spatial precipitation values, the Generate Earth Systems Science input model (GENESYS) applies a monthly spatial correction determined using monthly precipitation values also derived from PRISM (see MacDonald et al. 2009). Precipitation estimates were validated using only SWE data which were available for all of the snow surveys as well as the Limestone Ridge and Southesk snow pillows. Given SWE represents the amount of water within a snowpack, it was assumed that SWE provides a reasonable surrogate for accumulated precipitation over the winter.

3.3 Hydrometeorological Model

The GENESYS hydrometeorological model was applied to assess potential changes in mountain snowpack in the upper North Saskatchewan River watershed in response to General Circulation Model (GCM)-derived scenarios of future climate. The GENESYS model has successfully simulated snow water equivalent (SWE) for both the St. Mary (MacDonald et al. 2009) and Oldman River watersheds (Lapp et al. 2005).

The GENESYS model integrates a geographic information system (GIS) and a series of physical subroutines to estimate hydrometeorological variables at high spatial resolution on a daily time step over the study watershed. To apply the physical subroutines spatially, the GENESYS model is linked to terrain categories (TCs) derived using a GIS. TCs for the upper North Saskatchewan River watershed were derived from a GIS overlay analysis of sub-watershed boundaries, 100 m elevation bands, and nine land cover types available from the *Circa 2000 Land Cover* dataset (National Land and Water Information Service 2008). This results in 997 individual TCs ranging in area from 100 m^2 to 1.6 km^2. For each TC, mean slope, aspect, and elevation values were derived. The physiographical characteristics of each TC were used as parameters in determining the hydrological balance.

The daily hydrological balance was calculated for each TC using Eq. 1, which represents the hydrological balance when snow is present:

$$SWE_{(t)} = SWE_{(t-1)} + P_{(t)} - I_{(t)} - S_{(t)} - R_{(t)} - IF_{(t)} \tag{1}$$

where *SWE* is the snow water equivalent (mm), *P* is simulated daily precipitation (rain or snow; mm), *I* is canopy interception (mm), *S* is sublimation (mm), *R* is runoff (mm), *IF* is infiltration (mm) and *t* is the time step (days). If the snowpack is completely removed, the hydrological balance is calculated using Eq. 2 to account for evapotranspiration (*ET;* mm), and soil moisture conditions (*SM;* mm):

$$SM_{(t)} = SM_{(t-1)} + P_{(t)} - I_{(t)} - ET_{(t)} - R_{(t)}, \tag{2}$$

The phase of precipitation is defined using a rain/snow partitioning algorithm derived by Kienzle (2008), which applies a sine curve and mean daily and threshold air temperatures to determine the proportions of rain and snow. Snow interception is calculated based on

Hedstrom and Pomeroy (1998), using Leaf Area Index (LAI) from the MODIS LAI dataset (Land Processes Distributed Active Archive Center 2008) and air temperature. Rain interception is calculated empirically from Von Hoyningen-Huene (1983). Sublimation is calculated as per Déry et al. (1998), which accounts for changes in snow and atmospheric conditions. Sublimation is estimated for both open and forested areas; however, in forested portions of the watershed estimates are only made in the canopy, as we assume relatively low sub-canopy atmospheric turbulence (Oke 1987). The inputs to the sublimation routine calculated in the GENESYS model include total incident radiation (W m^{-2}), daily average air temperature, relative humidity (%), and wind speed (m s^{-1}). Total incident radiation is calculated using the Arc GIS solar radiation tool (ESRI 2008). Relative humidity values are calculated using the method described by Glassy and Running (1994), where the dew point temperature is assumed to equal the daily minimum air temperature. A mean 10 m wind speed of 15 m s^{-1} is used for the calculation of sublimation, as this was the wind speed used by Déry et al. (1998) and resulted in reasonable estimates of sublimation when used by MacDonald et al. (2009).

Snowmelt is calculated using a temperature-index melt routine developed by Quick and Pipes (1977). The melt factor used in the snowmelt routine was calibrated using snow pillow data to 2.2 mm day^{-1} °C^{-1}, and assumed constant over the simulation period. The assumption of a static melt factor is not physically based, and may therefore limit future applications. However, given the data availability of the North Saskatchewan River watershed, it is not feasible to calculate the snow melt energy balance; thus, the routine used in this simulation is considered suitable for this application. Debele et al. (2010) also demonstrated that temperature-index methods are suitable when data are limiting. The effects of a static melt factor are minimized by only allowing melt to occur once the snowpack cold content reaches zero (MacDonald et al. 2009).

Soil infiltration is calculated as a proportion of daily snowmelt and rainfall, until saturation is reached; saturation values vary spatially depending on soil characteristics. Spatial soil characteristic were defined using a GIS overlay analysis with unpublished soils data from Banff National Park, Alberta provided by Parks Canada (A. Buckingham, pers. comm.) and land cover type. For each land cover type, mean soil depth and porosity were averaged and subsequently extrapolated over the watershed. Evapotranspiration was calculated based on a modified Penmann-Monteith method developed by Valiantzas (2006). Runoff is generated following complete soil saturation (i.e., some proportion of snowmelt and/or rainfall exceeds the soil water holding capacity). Although runoff is calculated, GENESYS does not incorporate runoff routing capabilities due to the complexities of defining the sub-surface characteristics of mountain watersheds (Magruder et al. 2009). Thus runoff output was not used in this analysis.

3.4 GENESYS Model Verification

Verification of air temperature simulations was completed using linear regression between simulated and observed daily air temperature values at sites AB 0, AB 1 and AB 5. SWE simulations were verified using both snow survey and pillow data, using linear regression to determine the performance of the SWE model at each of the eight sites within the watershed (Fig. 1). SWE variation at snow survey sites was modelled on a daily time step, enabling direct comparison of modelled SWE to snow survey measurements on the sampling date. The two snow pillow records provided an additional test of the ability of the model to simulate daily SWE values.

MODIS snow cover data were used to determine the model's ability to simulate snow cover extent (Hall et al. 2007). While MODIS data (500 m x 500 m) were available every 8 days from July 4, 2002 to the present, we used only spring (March, April, May) days with<5 % cloud

cover. Simulated SWE values from GENESYS were interpolated to a 500 m x 500 m grid for comparison with the MODIS dataset. The goodness of fit between modelled and simulated snow cover extent was calculated with the Hassen-Kuipers skill score (KSS), which results in a range of values between -1 and 1, where 1 is a perfect fit (Woodcock 1976).

3.5 Climate Change Scenarios

Future climate scenarios were selected using a method developed by Barrow and Yu (2005). The objective was to select a range of scenarios to capture possible future changes in temperature and precipitation. As seasonal changes are more variable than annual changes, Barrow and Yu (2005) suggest that the season of interest be used for future climate scenario selection. Since spring is the most important season in terms of the timing of both maximum snow accumulation and onset of snow ablation, this season was used to select future climate scenarios for this study. Using the Barrow and Yu (2005) method, 2050 spring predictions of temperature and precipitation change are plotted for forty General Circulation Models (GCMs) and emissions scenarios (Fig. 3). Each point represents a specific GCM prediction of change in global mean air temperature and precipitation relative to the1961 to 1990 historical normal period for emissions scenarios defined by IPCC (2007), and available from the Pacific Climate Impacts Consortium (PCIC 2009). Five scenarios were selected for this study: four representing extreme changes in spring 2050 air temperature and precipitation, one representing median change. The scenarios are: BCCR (A2), CGCM (B1), MIRO (A1B), NCAR (A1B), and NCAR (B1) (Table 4).
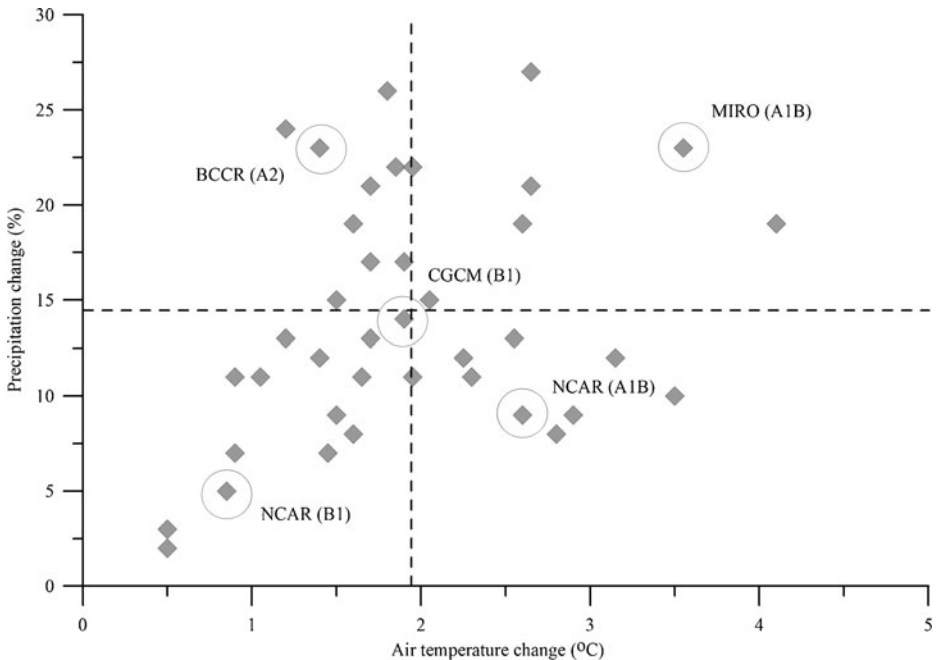
Fig. 3 Plot of air temperature and precipitation change for spring 2050 (relative to the 1960-91 average). Circled points indicate the selected future climate scenarios, and dashed lines represent the median of all scenarios. The first four letters of the future climate scenario represent the GCM, while letters and numbers in brackets represent the emissions scenario

Table 4 Seasonal changes in basin average air temperature (°C) and precipitation (%) for all five climate change scenarios

		Fall		Winter		Spring		Summer	
		Temp	Precip	Temp	Precip	Temp	Precip	Temp	Precip
2020s	BCCR (A2)	0.9	5.0	0.5	7.0	0.3	−2.0	0.6	2.0
	CGCM (B1)	1.1	14.0	1.6	10.0	0.6	5.0	1.3	9.0
	MIRO (A1B)	1.6	8.0	1.8	3.0	2.1	8.0	2.2	−4.0
	NCAR (A1B)	2.1	1.0	2.4	7.0	1.3	2.0	2.4	−4.0
	NCAR (B1)	2.15	1.0	3.2	10.0	0.9	5.0	1.5	0.0
2050s	BCCR (A2)	1.5	−1.0	1.4	13.0	1.4	23.0	1.4	−3.0
	CGCM (B1)	1.7	14.0	2.4	14.0	1.9	14.0	1.9	7.0
	MIRO (A1B)	3.3	16.0	3.9	9.0	3.6	23.0	4.2	−16.0
	NCAR (A1B)	2.7	9.0	3.5	14.0	2.6	9.0	3.9	4.0
	NCAR (B1)	2.1	4.0	2.3	12.0	0.9	5.0	2.5	2.0
2080s	BCCR (A2)	2.9	16.0	2.6	13.0	1.6	28.0	3.5	−1.0
	CGCM (B1)	1.8	28.0	2.4	28.0	1.9	19.0	2.3	6.0
	MIRO (A1B)	4.7	20.0	5.6	29.0	6	24.0	6	−15.0
	NCAR (A1B)	3.4	12.0	5	11.0	3	15.0	4.8	14.0
	NCAR (B1)	2.5	5.0	3.5	12.0	1.5	20.0	2.9	1.0

3.6 Downscaling GCM Temperature and Precipitation Changes

The 'delta' method of downscaling uses projected monthly changes in air temperature (dT) and precipitation (dP) based on results from each selected scenario (Table 4) to shift the observed 1961 to 1990 climate record, and has been used in a number of hydrological impacts studies (Hamlet and Lettenmaier 1999; Morrison et al. 2002; Andreasson et al. 2004; Loukas et al. 2004; Lapp et al. 2005; Cohen et al. 2006; Merritt et al. 2006). The key limitation of this method is that—although the local historical variability of the climate stations used to run the model is preserved (Hamlet and Lettenmaier 1999)—it does not explicitly account for changes in the variability of future climatic conditions (Leavesley 1994). The advantage to the delta method, however, is that it's simple and allows for inter-study comparison. Given the uncertainty in future climate variability, this method of incorporating historical variability provides useful estimates of the impacts of climate change on water resources.

The GENESYS model was driven using daily air temperature and precipitation values adjusted for the range of future climate scenarios selected. For each of the 1961 to 1990 input files, air temperature and precipitation changes were applied based on the scenarios chosen. Given that daily estimates of future air temperature changes are not available, a Fourier transform was applied to the future monthly maximum and minimum air temperature data from the GCM scenarios (Epstein and Ramirez 1994; Morrison et al. 2002). The resulting daily values of absolute air temperature change were used to perturb daily air temperature values from the 1961 to 1990 period. Percent changes in precipitation were also calculated for the GCM output relative to the 1961 to 1990 period. Daily precipitation values from 1961 to 1990 were adjusted by the percent change for the future period as provided in Table 4. New 30-year datasets representing changes in air temperature and precipitation predicted by the GCMs for the 2020s (2010 to 2039), 2050s (2040 to 2069) and 2080s (2070 to 2099) were used as input to the GENESYS model to output 15 simulations of future hydrometeorological conditions (three time periods and five GCM scenarios) in the upper North Saskatchewan River watershed.

4 Results and Discussion

4.1 Air temperature Verification

The calibrated lapse rates provide good air temperature estimates at a daily time step (Figs. 4, 5 and 6), although accuracy decreases with increasing elevation. This is likely a function of increasing distance from the driver stations and increasing air temperature variability in high elevation mountainous terrain. The decrease in simulation accuracy with elevation is expected given the spatial scale of the study region and the limited availability of high elevation air temperature records.

4.2 SWE Verification

SWE simulations compared well with snow course data for the eight snow course sites (Fig. 7; r^2=0.78, p<0.0001, RMSE=106.0 mm, n=614). Mean SWE values for all dates simulated did not differ significantly between simulated and observed: observed mean SWE was 238.2 mm and simulated mean SWE was 232.2 mm (t-stat=0.48, p=0.62). These results demonstrate that, overall, mean SWE across the watershed can be simulated by the GENESYS model. However, there is substantial scatter in the data, and modeled values show greater variability than observed SWE. The most likely source of this error is the difference in spatial scale between the simulations and the snow surveys. TCs used in the GENESYS model range from 100 m^2 to 1.6 km^2, while snow survey measurements are typically collected at the 100–500 m scale. The model is thus less able to account for the local characteristics of snow course sites which are affected by highly variable, site-specific physiographic conditions (Julander and Bricco 2006).

Comparison of daily observed SWE values from Limestone Ridge with simulated values showed 4 years (2002, 2003, 2006, and 2007) where SWE values compared very well (Fig. 8), 1 year (2005) where SWE was substantially under simulated, and 1 year (2004) where SWE was substantially over simulated. However, overall the simulation was good (r^2=0.71, p<0.0001, RMSE=42.7 mm).
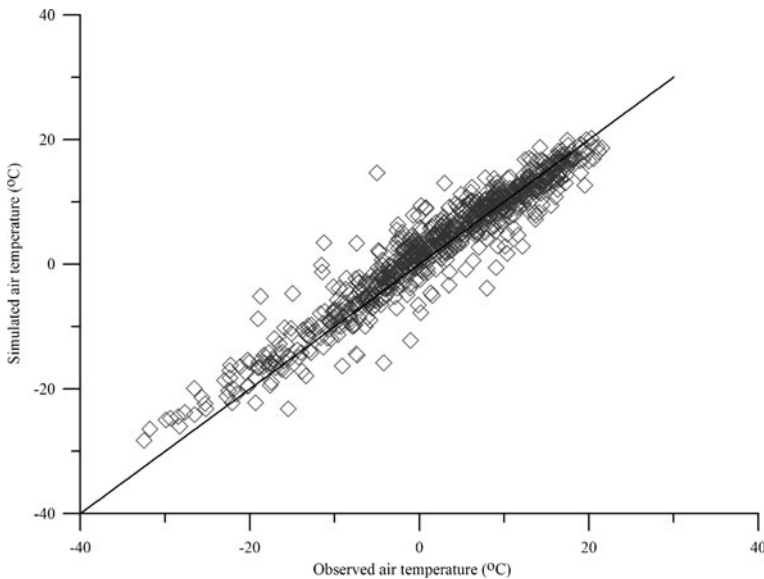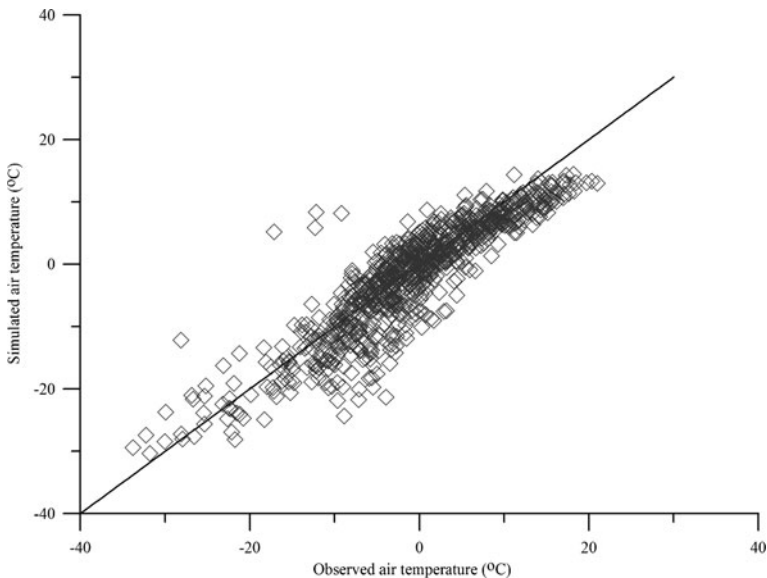

Fig. 4 Observed vs. simulated daily air temperature (r^2=0.91, p<0.001, RMSE=2.8 °C, n=831) at the AB 0 site (1070 m). The line represents the 1:1 line
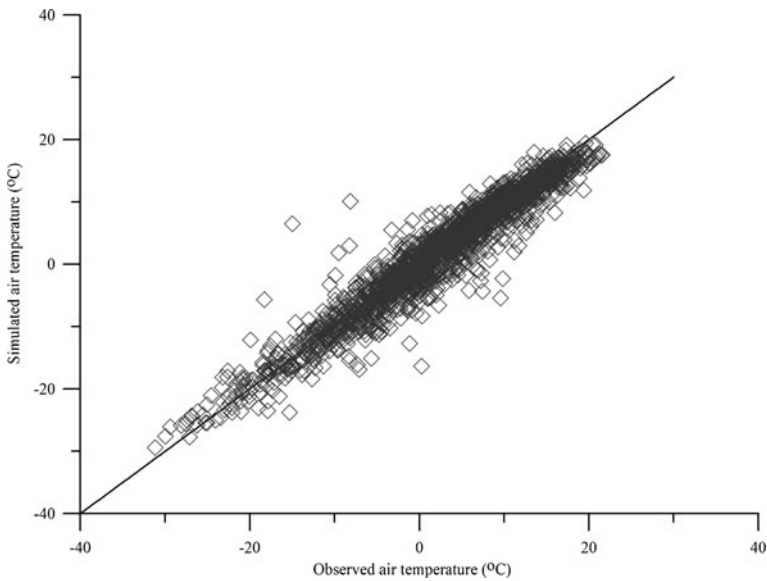
**Fig. 5** Observed vs. simulated daily air temperature Observed vs. simulated daily air temperature (r^2=0.93, p<0.001, RMSE=2.5 °C, n=1929) at the AB 1 site (1280 m). The line represents the 1:1 line

The simulated and observed datasets at the Southesk snow pillow did not compare as well as at the Limestone Ridge snow pillow (Fig. 9): 2007 and 2008 represent an over- and under-simulation, respectively (r^2=0.62, p<0.0001, RMSE=78.5 mm). The poor simulations in specific years at both snow pillows are likely a function of local variability in inter-annual hydrometeorological conditions that are not captured by the model. The meteorological

Fig. 6 Observed vs. simulated daily air temperature (r^2=0.80, p<0.001, RMSE=3.9 °C, n=876) at the AB 5 site (2120 m). The line represents the 1:1 line
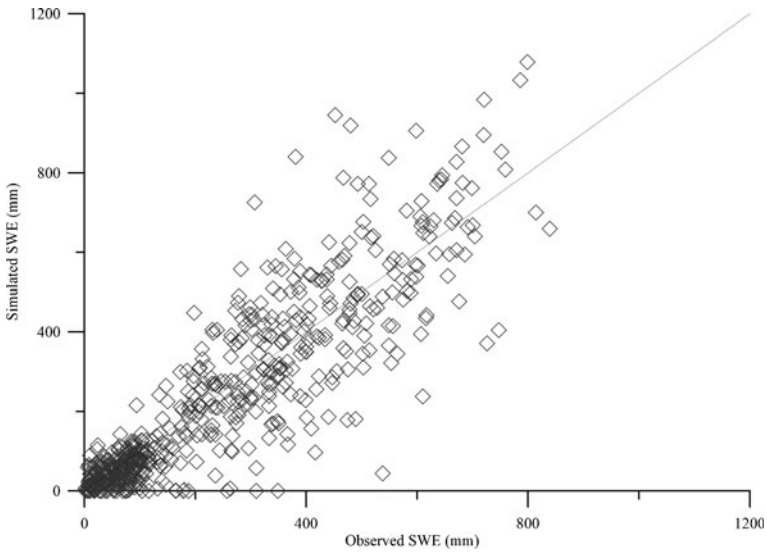
Fig. 7 Observed vs. simulated SWE (mm) for all snow courses. Observed values are SWE recorded during each snow survey, conducted in March, April and May from 1977 to 2008

stations used to drive the model are located in valley bottoms far from the snow pillow stations used to test the model. Given this spatial distribution of input data, GENESYS simulations of snow course and snow pillow measurements are reasonable.

Simulated snow cover extent compared well with MODIS data for the image dates selected (Table 5), with KSS values ranging from 0.30 to 0.67. The best and worst simulated dates (March 30, 2007 and May 17, 2008, respectively) are shown in Fig. 10. On both dates, the simulation misrepresents snow extent in the eastern, less topographically diverse portion of the watershed, with no snow predicted by the model where MODIS shows snow covered pixels. In the mountainous portion of the watershed, where snow accumulation is higher, the model appears to more realistically represent snow extent. Thus the model is able to simulate spatial SWE during the peak accumulation period with reasonable accuracy, providing
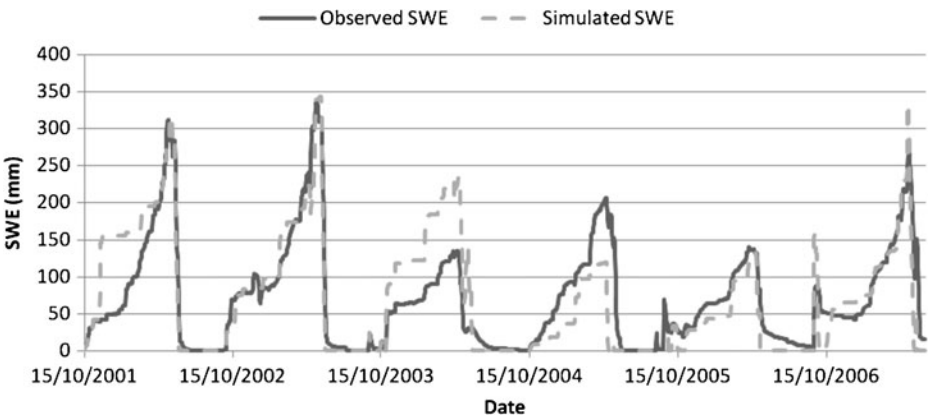
Fig. 8 Observed and simulated SWE at the Limestone Ridge snow pillow (1950 m)
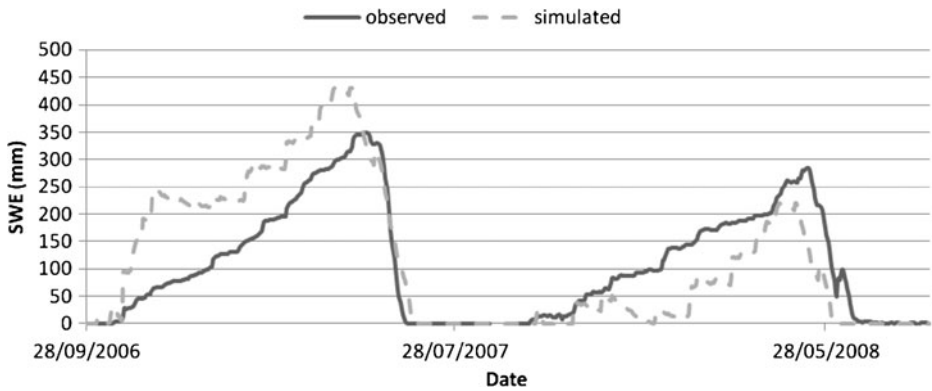
Fig. 9 Observed and simulated SWE at the Southesk snow pillow (2200 m)

confidence in models ability to simulate spatial snow extent during the critical spring period in the North Saskatchewan River watershed.

4.3 Potential Future Changes in Watershed-Scale SWE

4.3.1 Watershed-Average SWE

There is no significant difference in basin wide maximum SWE averaged over the watershed between the historical (1961 to 1990) period and future predictions, with the exception of simulations using the CGCM (B1) 2080 and NCAR (A1B) 2080 future climate scenarios (Table 6). Basin average maximum SWE simulated with the CGCM (B1) future climate scenario shows a significant increase, while simulations using the NCAR (A1B) scenario show a significant decrease. Stewart (2009) suggests that increases in cold-season precipitation could mask the effects of climate warming until: (a) warming is large enough to outweigh the effect of increased precipitation, or (b) precipitation increases are no longer occurring, at which time mountain snowpack may experience a step-like change. This could be important for the North Saskatchewan watershed, as it is unknown when these air temperature and precipitation thresholds will be reached.

Table 5 Summary of KSS and% correct snow covered area of simulated vs MODIS

Date	KSS	%Correct
17-May-04	0.45	75
7-Apr-05	0.45	65
15-Apr-05	0.54	75
25-May-05	0.55	82
15-Apr-06	0.57	80
17-May-06	0.40	88
30-Mar-07	0.67	79
9-May-07	0.56	80
25-May-07	0.53	77
17-May-08	0.30	82
25-May-08	0.35	86
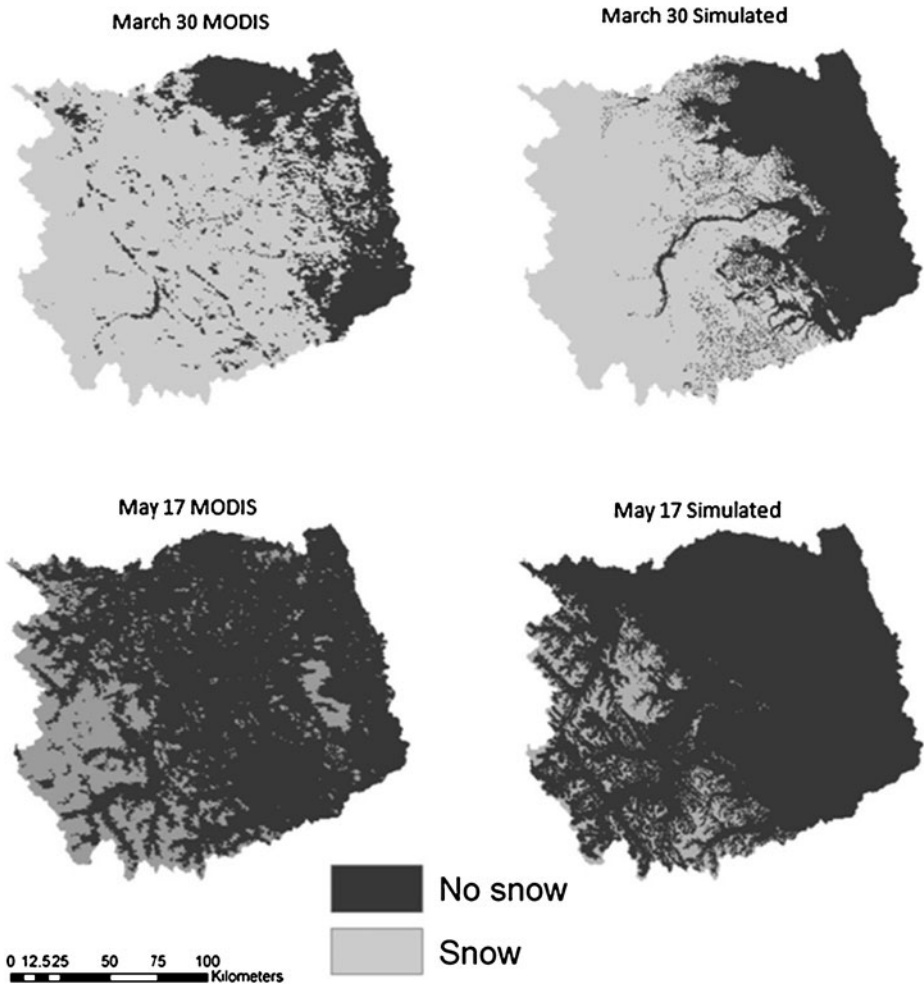
Fig. 10 Simulated snow covered area and MODIS snow covered area comparisons for the best and worst simulated dates: March 30, 2007 and May 17, 2008

4.3.2 Elevation Dependent Changes in SWE

A key hydrometeorological threshold in mountain environments is the elevation of the zero degree isotherm. The zero degree isotherm provides important information about the potential future changes in mountain snowpack, as SWE becomes more sensitive to air temperature with atmospheric warming (Mote 2006). For example, at low to moderate elevations in the western United States, winter precipitation shifted significantly from snow- to rain-dominated from 1949 to 2004 (Knowles et al. 2006). The historical zero degree isotherm in the North Saskatchewan watershed is 2200 m (Fig. 11); GENESYS simulations predict that the elevation of this isotherm would shift upward under all future climate scenarios (Fig. 11). The least change is predicted to occur under the CGCM (B1) scenario, where the zero degree isotherm would only move to 2500 m by the 2080s. The greatest change is under the MIRO (A1B) scenario, where the isotherm is predicted to shift to 3000 m by the 2080s. We focus on these two extreme scenarios to examine potential changes in precipitation phase as a function of elevation, and subsequent effects on the timing of snow accumulation and ablation.

Table 6 Comparison of maximum SWE for each 30 year time period relative to the historical (1961 to 1990) period. Bolded mean values indicate significant changes at the 95 % confidence level

		Historical	2020s	2050s	2080s
BCCR (A2)	Mean	69.3	75.3	73.4	70.1
	Standard deviation	22.4	24.8	26.3	30.9
CGCM (B1)	Mean	69.3	77.2	75.3	**83.7**
	Standard deviation	22.4	24.8	26.4	30.0
MIRO(A1B)	Mean	69.3	69.2	63.5	64.1
	Standard deviation	22.4	26.1	28.7	36.2
NCAR(A1B)	Mean	69.3	62.6	61.7	**51.6**
	Standard deviation	22.4	28.1	32.9	32.4
NCAR(B1)	Mean	69.3	68.1	67.1	58.8
	Standard deviation	22.4	35.7	31.4	32.9

Associated with predicted increases in air temperature is a shift in the 30-year watershed average snow line (lowest elevation of perennial snow cover) in both the CGCM (B1) and MIRO (A1B) scenarios. The historical simulated snow line is 2700 m. In the CGCM (B1) scenario 30-year watershed average elevation of the snow line increases to 2800 m, 2900 m and 3100 m for the 2020, 2050 and 2080 periods respectively. Simulations using the MIRO (A1B) scenario predict a shift to 3100 m by the 2020 period and no perennial snow cover for the 2050 and 2080 periods.
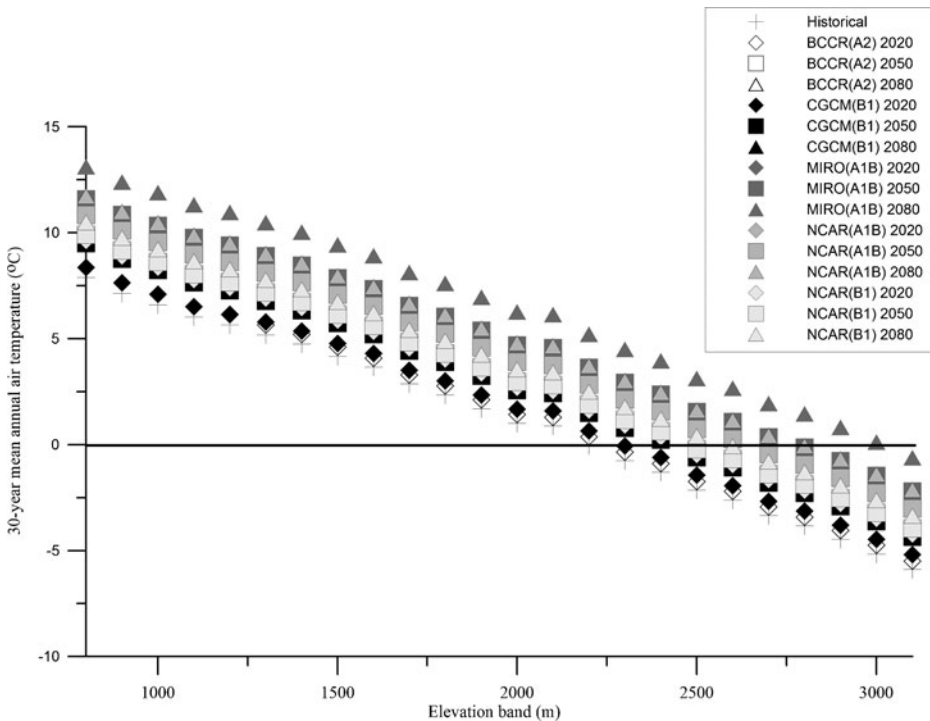
Fig. 11 30-year mean annual air temperature plotted against elevation for the historical, BCCR(A2), CGCM (B1), MIRO(A1B), NCAR(A1B), and NCAR(B1) future climate scenarios. The thick black line indicates the zero degree isotherm
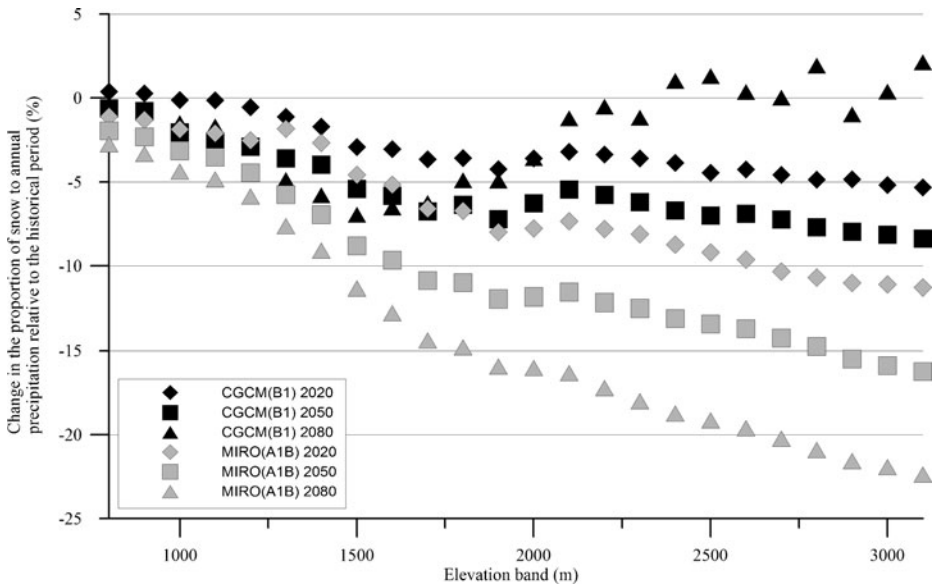
Fig. 12 Change in the proportion of snow as a percentage of annual precipitation for the CGCM(B1) and MIRO(A1B) 2020, 2050, and 2080 future climate scenarios, all relative to the historical (1961 to 1990) period. Future SWE amounts remain near historical normal due to substantial increases in winter precipitation under all future scenarios (see Table 3)

The shift towards warmer air temperatures at higher elevations would change a proportion of winter precipitation from snow to rain, with the greatest changes occurring at higher elevations (Fig. 12). The historical (1961 to 1990) proportion of winter precipitation falling as snow at 2200 m (zero degree isotherm) was estimated to be 60 %. Future predictions for the CGCM (B1) scenario at 2200 m result in reductions of the proportion of winter precipitation falling as snow to 56 %, 54 % and 59 % for the 2020, 2050, and 2080 periods respectively. The MIRO (A1B) scenario predicts reductions of the proportion of winter precipitation falling as snow to 52 %, 47 %, and 42 % for the 2020, 2050, and 2080 periods respectively. These results demonstrate that under the CGCM (B1) and MIRO (A1B) scenarios, air temperature thresholds for rain to occur are reached where air temperatures have historically remained below this threshold. An exception is the CGCM (B1) scenario for the 2080 time period, where there is only a 1 % change in the proportion of winter precipitation falling as snow at 2200 m. A 19 to 28 % increase in spring, fall and winter precipitation is not offset by a 1.8 to 2.4 °C change in air temperature (Table 4).

4.3.3 Timing of Spring Snowmelt

An earlier onset of spring snowmelt has been recorded in studies across western North America (Burn 1994; Cayan et al. 2001; Mote et al. 2005; Regonda et al. 2005; Stewart et al. 2005; Clow 2010; Gillian et al. 2010), and is likely to result in a longer summer drought season in regions supported by snowmelt runoff (Stewart 2009). With water demand expected to increase due to human population growth, a longer summer drought season could have important implications for ecosystems and human water users in the North Saskatchewan watershed. Therefore, understanding how and where the timing of peak SWE and snowpack removal may change in the future is important for water management in this watershed.

The date of maximum SWE is important as this represents the time at which spring snowmelt begins, as after this date SWE begins to decline. The CGCM (B1) future climate
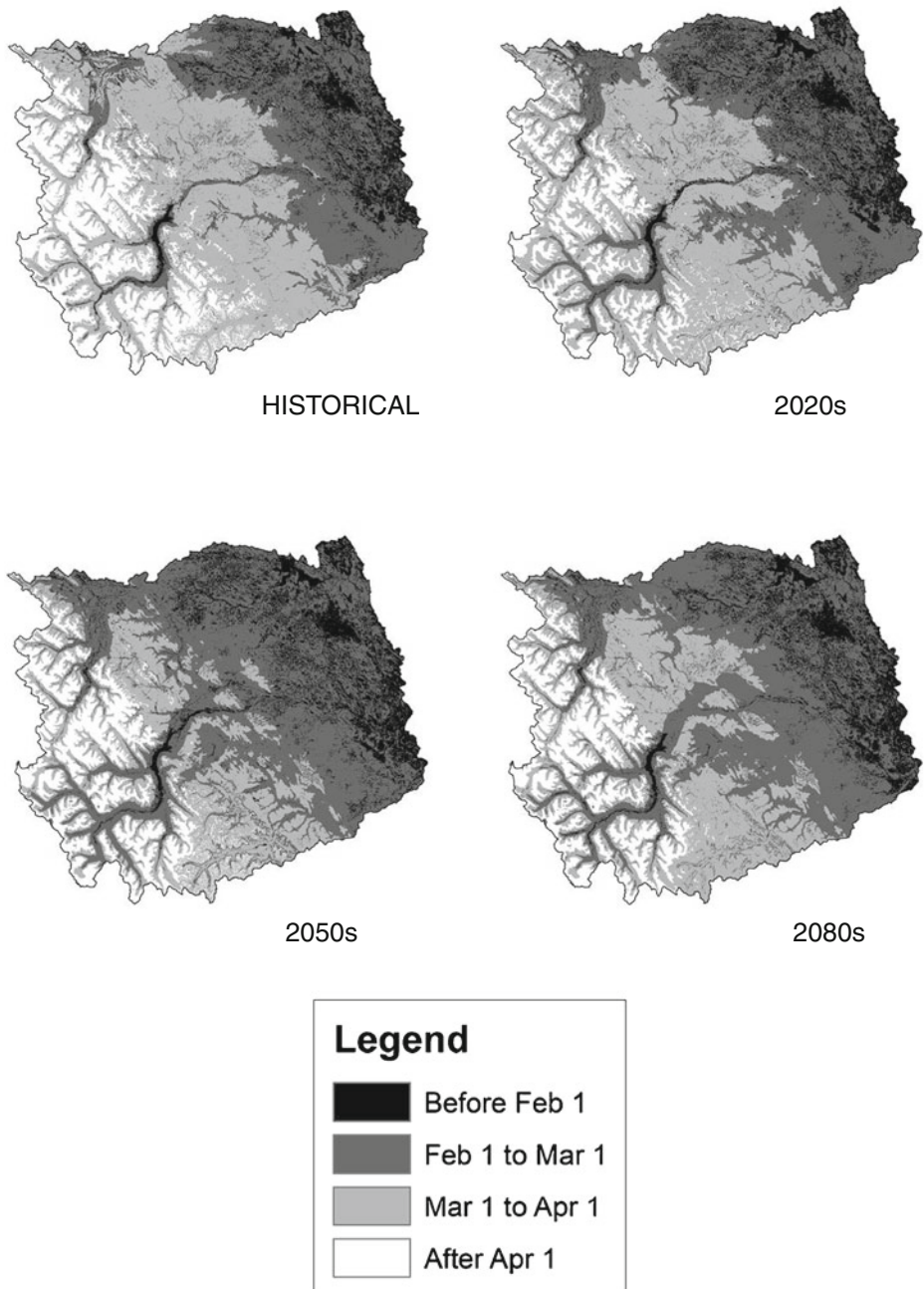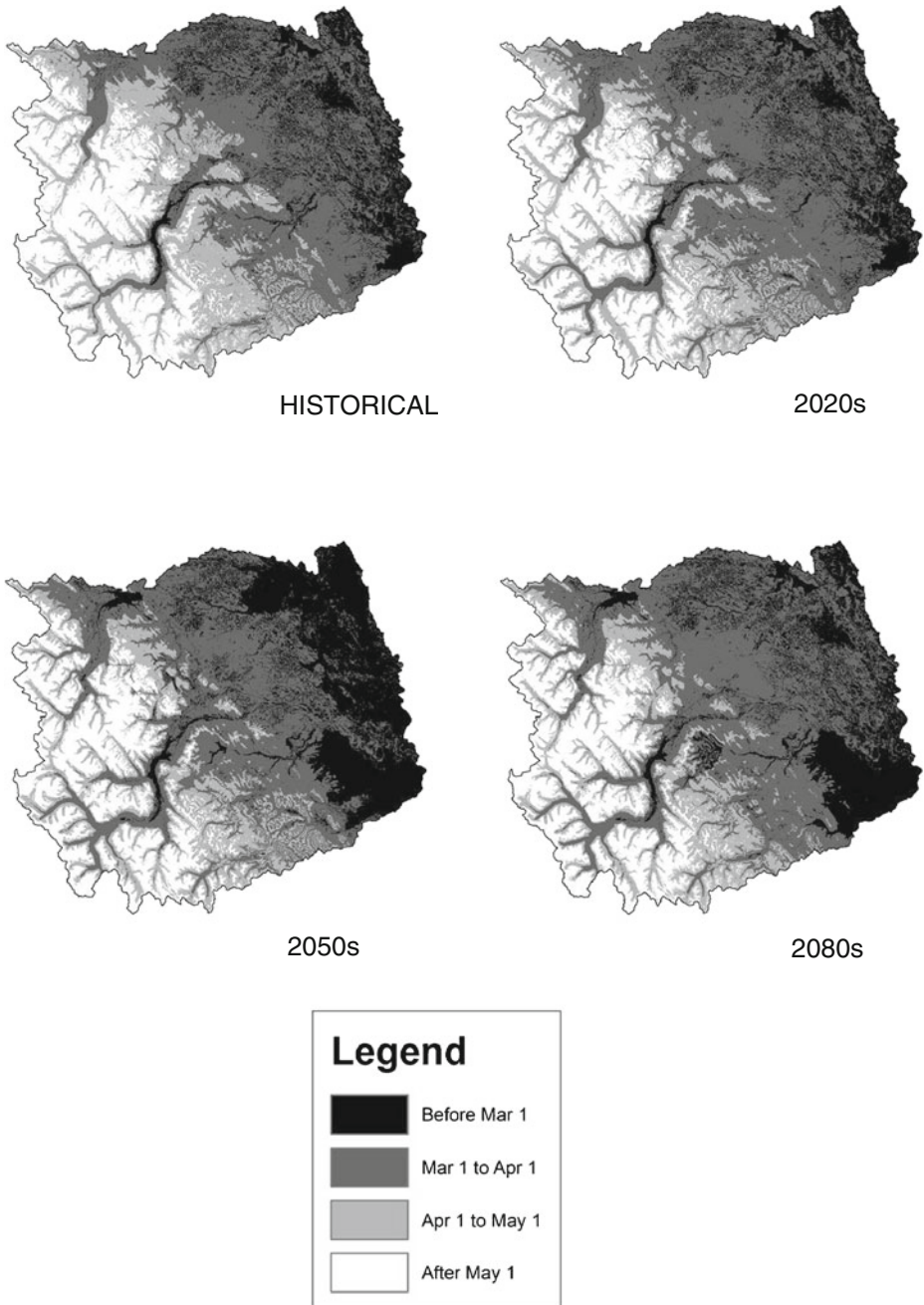
Fig. 13 The 30-year mean date of maximum SWE for the historical (1961 to 1990), 2020, 2050, and 2080 periods for the CGCM(B1) future climate scenario

scenario is predicted to result in minimal spatial change in the date of maximum SWE, with the greatest shift occurring at mid-elevations (Figs. 13 and 14). In contrast to CGCM (B1), the MIRO (A1B) scenario shows substantial spatial change in the date of maximum SWE which
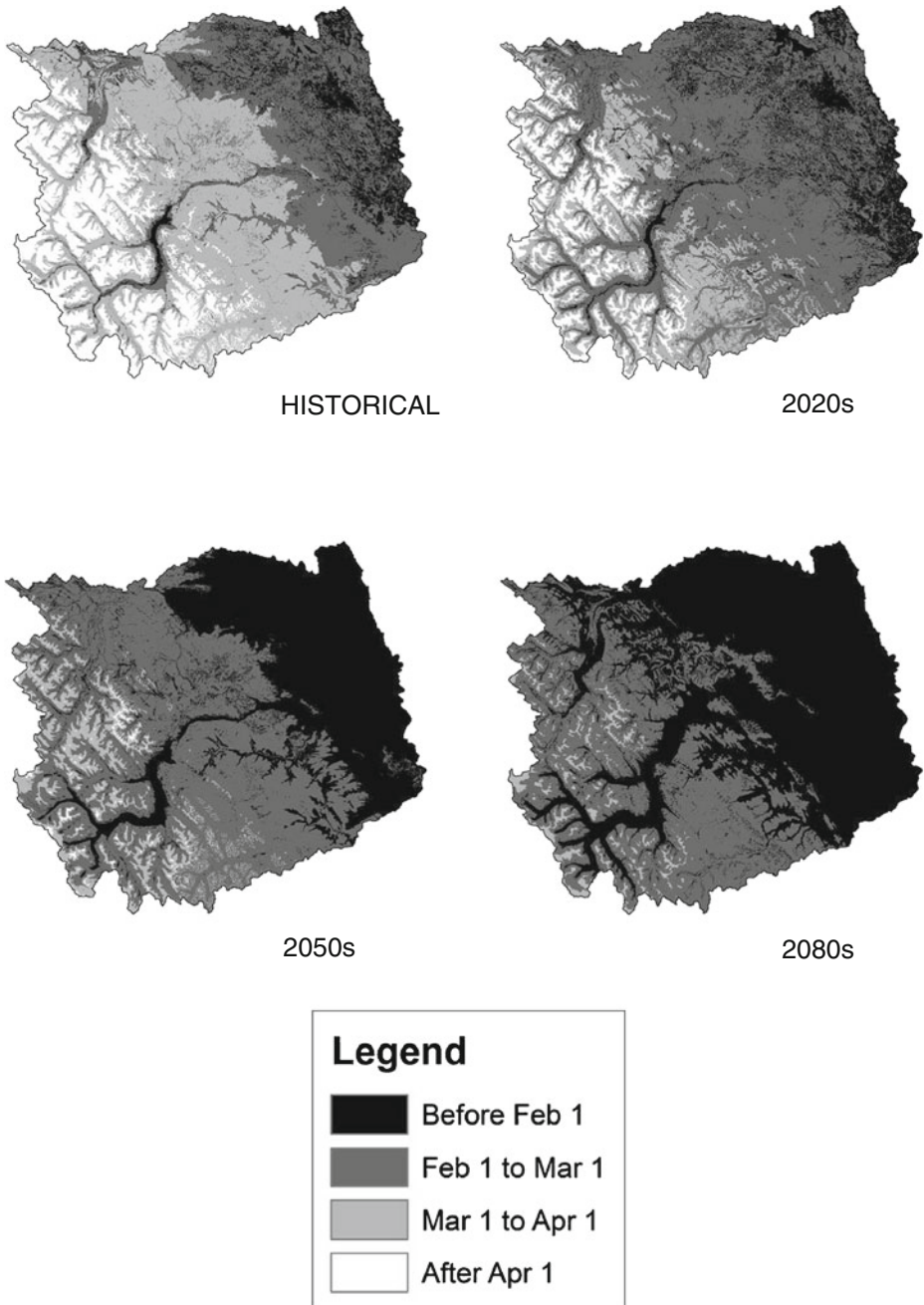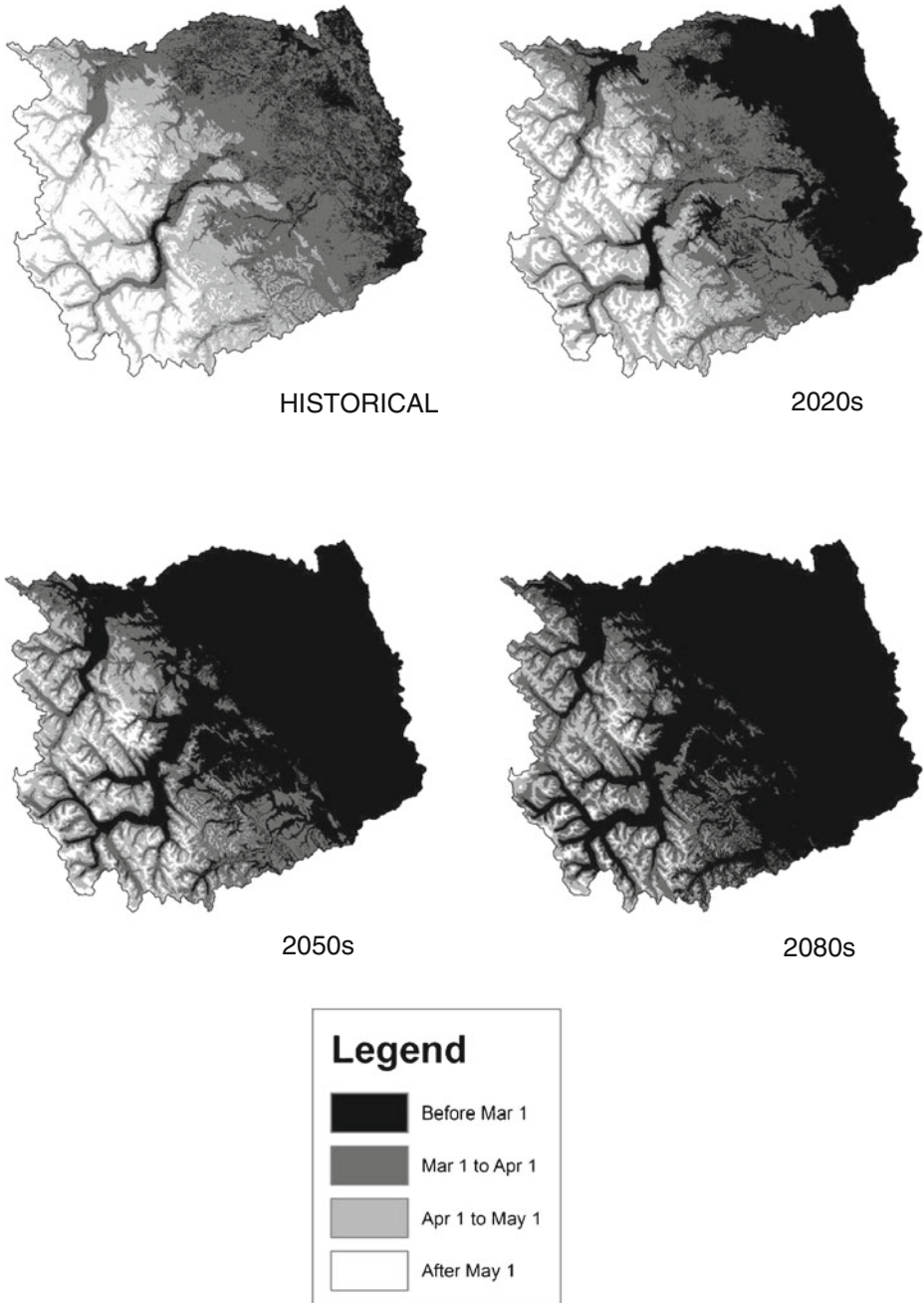
Fig. 14 The 30- year mean date of maximum SWE for the historical, 2020, 2050, and 2080 periods for the MIRO(A1B) future climate scenarios

occurs by March 1 across 97 % of the watershed in the 2080 period (Fig. 13). This shift towards earlier peak SWE relative to the historical (1961 to 1990) date of April 2 is primarily a function of the large air temperature increases predicted by the MIRO (A1B) scenario.

Fig. 15 The 30-year mean date of complete snow removal for the historical, 2020, 2050, and 2080 periods for the CGCM(B1) future climate scenarios. Where complete snow removal does not occur (i.e. higher elevations), the date of minimum SWE is used

As with the date of maximum SWE, the CGCM (B1) scenario does not result in substantial spatial changes in the date of minimum SWE, but shows a shift towards potentially later dates of

Fig. 16 The 30-year mean date of complete snow removal for the historical, 2020, 2050, and 2080 periods for the MIRO(A1B) future climate scenarios. Where complete snow removal does not occur (i.e. higher elevations), the date of minimum SWE is used

minimum SWE at lower elevations (Figs. 15 and 16). This is largely a function of increased precipitation combined with relatively minimal air temperature change under this scenario. The

MIRO (A1B) scenario, however, shows 70 % of the watershed reaching minimum SWE before March 1, by the 2080 period. Also, only 1 % of the watershed is predicted to reach minimum SWE after May 1 by the 2080 period, where historically 17 % of the watershed reached minimum SWE after May 1.

The period between the date of maximum SWE and the date of minimum SWE, representing the rate of snowmelt demonstrates that air temperature plays a larger role in governing spring snow processes than does precipitation. For the historical (1961 to 1990) period, the average 30-year melt rate over the entire watershed was 37 days. For the CGCM (B1) scenario, the average rate of snowmelt is not predicted to change significantly for the 2020 (37 days; t-stat=−0.18; p=0.43), 2050 (38 days; t-stat=−0.13; p=0.47) or 2080 (38 days; t-stat=−0.18; p=0.42) periods. The MIRO (A1B) scenario, with greater air temperature increases is, however, predicted to result in no significant change in the 30-year average rate of snowmelt for the 2020 (35 days; t-stat=0.54; p=0.29) and 2050 (32 days; t-stat=1.15; p=0.12) periods with a significant change at the 90 % confidence level by the 2080 (31 days; t-stat=1.3; p=0.09) period.

The results from this study suggest projected air temperature increases, independent of changes in precipitation, would have a substantial effect on the proportion of winter precipitation falling as snow, the timing of maximum SWE, minimum SWE and the duration of the snowmelt period. This finding is consistent with current trends observed in the Pacific Northwest, where despite increases in precipitation, significant increases in air temperature are resulting in substantial declines in SWE (Mote 2003). Knowles et al. (2006) demonstrate the importance of air temperature controls on controlling the proportion of precipitation falling as snow, with a focus on the western United States. Here it is shown that even a cold, high latitude environment, changes in the proportion of precipitation falling as snow which have already been observed in lower latitudes are likely to occur. A shorter snow melt season, resulting from predictions of increased melt rates also demonstrates that air temperature outweighs the effect of increased precipitation.

5 Summary

The GENESYS model is able to simulate hydrometeorological processes over a large geographic region with minimal input data, although simulations could be improved with higher spatial and temporal resolution air temperature and precipitation data, particularly at higher elevations.

Simulations of future SWE suggest there may be little change in annual maximum snow accumulation over the entire North Saskatchewan River watershed. However, spring melt may occur earlier as evidenced by earlier dates of maximum SWE over the watershed. Shifts towards a higher elevation zero degree isotherm and an increase in the annual proportion of rain versus snow support the conclusion that air temperature changes affect the seasonal snowpack independently of precipitation changes.

The greatest change in the proportion of annual precipitation falling as snow in the North Saskatchewan River watershed under the CGCM (B1) and MIRO (A1B) future climate scenarios is expected to occur at higher elevations in the watershed, with the exception of the 2080 period for the CGCM (B1) scenario. This change is attributed to increased air temperatures above the threshold for precipitation to fall as snow rather than rain, where historically these thresholds were not reached at these elevations. Increased air temperature also results in spatial changes in the date of maximum and minimum SWE: substantial shifts towards earlier maximum and minimum SWE occur in the MIRO (A1B) scenario, which is much warmer than the CGCM (B1) scenario.

Shifts in the phase of precipitation and the timing of maximum and minimum SWE have important implications for water resource management. As other studies have shown, reliability and predictability of water supply is important to reservoir management. With a greater proportion of annual precipitation falling as rain, water storage in the snowpack would be reduced, reducing the predictability and reliability of this water supply. Earlier maximum and minimum SWE indicate a shift towards earlier spring onset in the future, which may result in dryer summer conditions with reduced late season water supply.

References

Alberta Environment (2009) 1973 to 2008 snow and air temperature data. Provided by John Pedlar and Rick Pikering of Alberta Environment.

Andreasson J, Lindstrom G, Grahn G, Johansson B (2004) Runoff in Sweden-mapping of climate change impacts on hydrology. Nord Hydrol Prog 48:625–632

Barnett TP, Adam JC, Lettenmaier DP (2005) Potential impacts of a warming climate on water availability in snow-dominated regions. Nature 438:1–7

Barnett TP, Pierce DW, Hidalgo HG, Bonfils C, Santer BD, Das T, Bala G, Wood AW, Nozawa T, Mirin AA, Cayan DR, Dettinger MD (2008) Human-induced changes in the hydrology of the western United States. Science 319:1080. doi:10.1126/science.1152538

Barrow E, Yu G (2005) Climate Change Scenarios for Alberta - A Report Prepared for the Prairie Adaptation Research Collaborative (PARC) in co-operation with Alberta Environment. Regina, Saskatchewan, 73

Beniston M (2003) Climatic change in mountain regions: A review of possible impacts. Clim Chang 59:5–31

Beniston M, Diaz HF, Bradley RS (1997) Climatic change at high elevation sites: an overview. Clim Chang 36:233–251

Booth E, Byrne JM, Jiskoot H, MacDonald R (2010) Modeling the response of glaciers to climate change in the upper North Saskatchewan River basin. *Eos Trans. AGU,* 91(52), Fall Meet. Suppl., Abstract GC51D-0788.

Burn DH (1994) Hydrologic effects of climate change in west-central Canada. J Hydrol 160:53–70

Cayan DR, Kammerdiener SA, Dettinger MD, Caprio JM, Peterson DH (2001) Changes in the onset of spring in the western United States. B Am Meteorol Soc 82:399–415

City of Edmonton (2010) Edmonton Population 1986-2006. City of Edmonton Planning and Development, using data from Statistics Canada. Accessed May 2010. http://www.edmonton.ca/business/documents/InfraPlan/edmonton_cma_population%281 %29.pdf

Clow DW (2010) Changes in the timing of snowmelt and streamflow in Colorado: A response to recent warming. J Climate 23:2293–2306

Cohen SJ (1991) Possible impacts of climate warming scenarios on water resources in the Saskatchewan River sub-basin, Canada. Clim Chang 19:291–317

Cohen SJ, Neilsen D, Smith S, Neale T, Taylor B, Barton M, Merritt W, Alila Y, Shepherd P, McNeil R, Tansey J, Carmichael J, Langsdale S (2006) Learning with local help: Expanding the dialogue on climate change and water management in the Okanagan region, British Columbia, Canada. Clim Chang 75:331–358

Daly C, Halbleib M, Smith JI, Gibson WP, Doggett MK, Taylor GH, Curtis J, Pasteris PA (2008) Physiographically-sensitive mapping of climatological temperature and precipitation across the conterminous United States. Int J Climatol 28:2031–2064

Debele B, Srinivasan R, Gosain AK (2010) Comparison of process-based and temperature-index snowmelt modeling in SWAT. Water Resour Manage 24:1065–1088

Déry SJ, Taylor P, Xiao J (1998) The thermodynamic effects of sublimating, blowing snow in the atmospheric boundary layer. Bound Lay Meteorol 89:251–283

Environment Canada (2010) Canadian Climate Normals 1971-2010. Accessed May 2010. http://www.climate.weatheroffice.gc.ca/climate_normals/results_e.html?Province=ALL&StationName=nordegg&SearchType=BeginsWith&LocateBy=Province&Proximity=25&ProximityFrom=City&StationNumber=&IDType=MSC&CityName=&ParkName=&LatitudeDegrees=&LatitudeMinutes=&LongitudeDegrees=&LongitudeMinutes=&NormalsClass=A&SelNormals=&StnId=2423&&autofwd=1

Epstein D, Ramirez JA (1994) Spatial disaggregation for studies of climatic hydrologic sensitivity. J Hydrol Eng 120:1449–1467

Flannigan MD, Amiro BD, Logan KA, Stocks BJ, Wotton BM (2005) Forest fires and climate change in the 21st century. Clim Chang 11:847–859

Gadd, B (1995) Handbook of the Canadian Rockies: Second edition. Corax Press: Jasper, Alberta. 831 pp.

Gillian BJ, Harper JT, Moore JN (2010) Timing of present and future snowmelt from high elevations in northwestern Montana. Wat. Resour. Res. 46: doi:10.1029/2009WR007861.

Glassy JM, Running SW (1994) Validating dirunal climatology logic of the MT-CLIM model across a climatic gradient in Oregon. Ecol Appl 4:248–257

Hall DK, Riggs GA, Salomonson VV (2007) updated weekly: MODIS/Aqua snow cover 8-day L3 Global 500 m grid V 005, [16 Oct, 2000; 17 Nov, 2000; 17 Jan, 2001; 14 Mar, 2001; 15 Apr, 2001; 17 May, 2001, 12 Jul, 2001; 14 Sept, 2001]. Boulder, Colorado USA: National Snow and Ice Data Center. Digital media.

Hamlet AF, Lettenmaier DP (1999) Effects of climate change on hydrology and water resources in the Columbia basin. J Am Water Resour As 35:1597–1623

Harma KJ, Johnson MS, Cohen SJ (2011) Future water supply and demand in the Okanagan basin, British Columbia: A scenario-based analysis of multiple, interacting stressors. Water Resour Manage. doi:10.1007/s11269-011-9938-3

Hedstrom NR, Pomeroy JW (1998) Measurements and modelling of snow interception in the boreal forest. Hydrol Process 12:1611–1625

Hicke JA, Jenkins JC (2008) Susceptibility of lodgepole pine to mountain pine beetle attack: Mapping stand structure across the western United States. For Ecol Manag 255:1536–1547

IPCC (2007) Climate Change 2007. In: Solomon S, Qin D, Manning M, Chen Z, Marquis M, Averyt KB, Tignor M, Miller HL (eds) The Physical Science Basis. Contribution of Working Group 1 to the Fourth Assessment Report of the Intergovernmental Panel on Climate Change. Cambridge University Press, Cambridge, United Kingdom and New York, NY, USA, p 996

Julander RP, Bricco M (2006) An examination of external influences embedded in the historical snow data of Utah, *Proceedings of the 74th Western Snow Conference*. Las Cruces, New Mexico, pp 67–78

Kienzle SW (2008) A new temperature based method to separate rain and snow. Hydrol Process 22:5067–5085

Knowles N, Dettinger MD, Cayan DR (2006) Trends in snowfall versus rainfall in the western United States. J Climate 19:4545–4559

Land Processes Distributed Active Archive Center (2008) LP DAAC, located at the U.S. Geological Survey (USGS) Earth Resources Observation and Science (EROS) Center (lpdaac.usgs.gov). Leaf Area Index - Fraction of Photosynthetically Active Radiation 8- Day L4 Global 1 km. Accessed December 2008.

Lapp S, Byrne JM, Kienzle SW, Townshend I (2005) Climate warming impacts on snowpack accumulation in an alpine watershed: a GIS based modeling approach. Int J Climatol 25:521–526

Leavesley GH (1994) Modelling the effects of climate change on water resources-A review. Clim Chang 28:159–179

Littell JS, McKenzie D, Peterson DL, Westerling AL (2009) Climate and wildfire area burned in western U.S. ecoprovinces, 1916–2003. Ecol Appl 19:1003–1021

Loukas A, Vasiliades L, Dalezios NR (2004) Climate change implications on flood response of a mountainous watershed. J Geophys Res 112:D11124. doi:10.1029/2006JD007561

MacDonald RJ, Byrne JM, Kienzle SW (2009) A physically based daily hydrometeorological model for complex mountain terrain. J Hydrometeorol 10:1430–1446

Magruder IA, Woessner WW, Running SW (2009) Ecohydrologic process modeling of mountain block groundwater recharge. Groundwater 47:774–785

Merritt WS, Alila Y, Barton M, Taylor B, Cohen S, Neilsen D (2006) Hydrologic response to scenarios of climate change in sub watersheds of the Okanagan basin, British Columbia. J Hydrol 326:79–108

Minville M, Brissette F, Krau S, Leconte R (2009) Adaptation to climate change in the management of a Canadian water-resources system exploited for hydropower. Water Resour Manage 23:2965–2986

Minville M, Brissette F, Krau S, Leconte R (2010) Behaviour and performance of a water resource system in Quebec (Canada) under adapted operating policies in a climate change context. Water Resour Manage 24:1333–1352

Morrison J, Quick MC, Foreman MGG (2002) Climate change in the Fraser River watershed: flow and temperature projections. J Hydrol 263:230–244

Mote PW (2003) Trends in snow water equivalent in the Pacific Northwest and their climatic causes. Geophys Res Lett 30. doi:10.1029/2003GL017258

Mote PW, Hamlet AF, Clark MP, Lettenmaier DP (2005) Declining mountain snowpack in western North America. B Am Meteorol Soc 86:39–49

North Saskatchewan Watershed Alliance (2005) State of the North Saskatchewan Watershed Report 2005: A foundation for collaborative watershed management. North Saskatchewan Watershed Alliance, Edmonton, Alberta. 202 pages.

Oke TR (1987) Boundary Layer Climates. Routledge, London, New York, p 435

Pacific Climate Impacts Consortium (2009) PCIC Regional Analysis Tool. Available at: http://pacificclimate.org/. Accessed Dec 2009.

Quick MC, Pipes A (1977) UBC Watershed Model. Hydrolog Sci Bull 306:215–233

Regonda SK, Rajagopalan B, Clark M, Pitlick J (2005) Seasonal cycle shifts in hydroclimatology over the western United States. J Climate 18:372–384

Rood SB, Samuelson GM, Weber JK, Wywrot KA (2005) Twentieth-century decline in streamflows from the hydrographic apex of North America. J Hydrol 81:1281–1299

Schindler DW, Donahue WF (2006) An impending water crisis in Canada's western prairie provinces. P Natl Acad Sci USA 103:7210–7216

Smith CD (2009) The relationship between monthly precipitation and elevation in the Canadian Rocky Mountain Foothills. *Proceedings of the 77th Western Snow Conference*, Canmore, Alberta, Canada, 37–46.

St. Jaques MJ, Sauchyn DJ, Zhao Y (2010) Northern Rocky Mountain streamflow records: Global warming trends, human impacts or natural variability? Geophys Res Lett 37:L06407. doi:10.1029/2009GL042045

Stewart IT (2009) Changes in snowpack and snowmelt runoff for key mountain regions. Hydrol Process 23:78–94

Stewart IT, Cayan DR, Dettinger MD (2004) Changes in snowmelt runoff timing in western North America under a 'business as usual' climate change scenario. Clim Chang 62:217–232

Stewart IT, Cayan DR, Dettinger MD (2005) Changes toward earlier streamflow timing across western North America. J Climate 18:1136–1155

ESRI (Environmental Systems Research Institute, Inc) (2008) ArcInfo (Version 9.3) [Computer software].

Transalta (2009) Our Plants. Retrieved April 25, 2009, from http://www.transalta.com.

Valeo C, Xiang Z, Bouchart FJ, Yeung P, Ryan C (2007) Climate change impacts in the Elbow River watershed. Can Water Resour J 32:285–302

Valiantzas JD (2006) Simplified versions for the Penman evaporation equation using routine weather data. J Hydrol 331:690–702

Von Hoyningen-Huene J (1983) Die Interzeption des Niederschlages in landwirtschaftlichen Pflanzenbeständen. Deutscher Verband für Wasserwirtschaft und Kulturbau 57:1–66

National Land and Water Information Service (2008) NLWIS *Data*. Retrieved September 10, 2008 from http://www4.arg.gc.ca/AAFC-AAC/display-afficher.do?id=1226330737632&lang=eng

Woodcock F (1976) The evaluation of yes/no forecasts for scientific and administrative purposes. Mon Wea Rev 104:1209–1214.

Zhang X, Harvey KD, Hogg WD, Yuzyk TR (2001) Trends in Canadian streamflow. Wat Resour Res 37:987–998